Volume Production of D^- Negative Ions in Low-Pressure D_2 Plasmas
- Negative Ion Densities versus Plasma Parameters -

Osamu Fukumasa and Shigefumi Mori

Department of Electrical and Electronic Engineering, Faculty of Engineering, Yamaguchi University, Tokiwadai 2-16-1, Ube, 755-8611, Japan

Abstract. Volume production of D^- negative ions including isotope effects is studied in a rectangular arc chamber. Production and control of plasma parameters in D_2 plasmas are performed by varying the intensity of the magnetic filter. The values of T_e and n_e in D_2 plasmas are slightly higher than ones in H_2 plasmas. T_e in D_2 plasmas cannot be decreased and is kept above 1 eV in the extraction region with the same MF intensity for optimizing H_2 plasmas. The stronger MF field is required for control of T_e in D_2 plasmas. Therefore, plasma production between H_2 and D_2 plasmas is different from each other. Namely isotope effect of plasma production is observed. H^- and D^- densities have different spatial distributions corresponding to those different plasma parameters. Extracted H^- and D^- currents are mainly determined by H^- and D^- densities in front of the extraction hole, respectively. According to the discussions based on estimated rate coefficient and collision frequency of main collision processes, it is reconfirmed that T_e in the extraction region should be reduced below 1 eV with n_e keeping higher for enhancement of H^- and D^- production. For studying enhancement of D^- production, preliminary results on VUV emission measurement is presented and discussed briefly.

1. Introduction

Sources of H^- and D^- negative ions are required for generation of efficient neutral beams with energies in excess of 150 keV. The magnetically filtered multicusp ion source has been shown to be a promising source of high-quality multiampere H^- ions. In pure hydrogen (H_2) discharge plasmas, most of the H^- ions are generated by the dissociative attachment of slow plasma electrons e_s (electron temperature $T_e \sim 1$ eV) to highly vibrationally excited hydrogen molecules H_2 (v”) (effective vibrational level v” ≥ 5-6). These H_2(v”) are mainly produced by collisional excitation of fast electrons e_f with energies in excess of 15-20 eV. Namely, H^- ions are produced by the following two step process [1, 2]:

$$H_2 (X^1\Sigma_g, v'' = 0) \quad + \quad e_f \quad \rightarrow \quad H_2^*(B^1\Sigma_u, C^1\Pi_u) \quad + \quad e_f', \qquad (1a)$$

$$H_2^*(B^1\Sigma_u, C^1\Pi_u) \quad \rightarrow \quad H_2 (X^1\Sigma_g, v'') \quad + \quad h\nu, \qquad (1b)$$

$$H_2 (v'') \quad + \quad e_s \quad \rightarrow \quad H^- \quad + \quad H. \qquad (2)$$

Production process of D^- ions is believed to be the same as that of H^- ions. To develop efficient D^- ion sources, namely to extract D^- ions with high current density, it is important to clarify production and control of deuterium (D_2) plasmas, and to understand difference in the two step process of negative ion production between H_2 plasmas and D_2 plasmas. Cesium seeding into this source is used to enhance negative ion currents and to reduce extracted electron currents. However, there are few studies on optimization of volume-produced D^- ions. Then, we focus on understanding the negative ion production mechanisms in the “volume” ion source where negative ions are produced in low-pressure pure H_2 or D_2 discharge plasmas.

For this purpose, we are interested in estimating densities of highly vibrationally excited molecules and negative ions in the source. The production process of H_2(v”)/D_2(v”) is discussed [3] by observing the photon emission, i.e. VUV emission associated with the process (1b) [4, 5]. To clarify the relationship between plasma parameters and volume production of negative ions, H^- or D^- ions in the source are measured [6, 7] by the laser photodetachment method [11].

In this paper, plasma parameter control by varying the magnetic field intensity of the MF is presented [8, 9]. Influence of these plasma parameter distributions on H^-/D^- production is discussed with using estimated rate coefficients and collision frequencies based on measured plasma parameters [9, 10]. Estimating negative ion densities in the source with the use of laser photodetachment technique, we discuss the relationship between negative ions in the source and extracted negative ion currents [8]. For studying enhancement of D^- production, preliminary results on VUV emission measurements are also presented.

2. Experimental set-up

Figure 1 shows a schematic diagram of the ion source [6-10]. The rectangular arc chamber is 25 cm × 25 cm in cross section and 19 cm in height. Four tungsten filaments with 0.7 mm in diameter and 20 cm in length are installed in the source region from side walls of the chamber. The line cusp magnetic field is produced by permanent magnets which surrounded the chamber. The external magnetic filter (MF) is composed of a pair of permanent magnets in front of the plasma grid (PG), and the MF separates the extraction region from the source region. PG potential is kept earth potential throughout the present experiments both for H_2 and D_2 plasmas.

In the source region, the VUV emission measurements related to the H_2(v") or D_2(v") production, i.e. the process (1b), are carried out by using the VUV spectrometer. The spectrometer was normally operated at a resolution of 0.1 nm.

Plasma parameters are measured by Langmuir probes. A magnetic deflection type ion analyzer is also used for relative measurements of the extracted H^- or D^- current. H^- or D^- densities in the source are measured by the laser photodetachment method [11]. A light pulse from a Nd:YAG laser (wavelength 1064 nm, duration of laser pulse 9 ns, repetition 10 Hz) is introduced from the side wall window of the chamber and passes through the source plasmas. The laser light axis can move across the MF.

3. Experimental results and discussion

3.1 Production and control of D_2 plasmas

On H^-/D^- volume production, desired condition for plasma parameters is as follows: T_e in the extraction region should be reduced below 1 eV while keeping n_e higher. To realize this condition, namely to enhance H^-/D^- production by dissociative attachment and to reduce H^-/D^- destruction by electron detachment including collisions with energetic electrons, the MF is used. For this purpose, plasma parameter control is studied by varying the intensity of the MF.

Figures 2 and 3 show axial distributions of plasma parameters (n_e and T_e) in H_2 and D_2 plasmas, respectively. By varying the intensity of the MF, axial distributions of n_e and T_e in both H_2 and D_2 plasmas are strongly changed in the downstream region (from z = 8 to -2 cm) [8-10]. Production and control of D_2 plasmas are almost the same characteristics as that of H_2 plasmas.

In Figs. 2 and 3, for the MF with 150 G (B_{MF} = 150 G), not only T_e but also n_e are decreased far from the MF, i.e. z = 8 cm, in the source region. On the other hand, decreases in n_e and T_e are shifted to downstream region for the case of 80 G and 60 G. Figure 4 shows the numerical results of trajectories for primary fast electrons corresponding to the same magnetic field configuration in the source shown in Fig. 1. With decreasing the intensity of the MF, location of fast electrons is extended to the extraction region. Namely, ionization collisions will occur more frequently in the downstream region and also increase n_e as shown in Figs. 2 and 3. In this source, due to the external MF, width of the half-maximum of magnetic field intensity is wider (about 16cm in this case) than the case of rod filter [5]. Namely, varying the intensity of the magnetic filter also indicates varying the strength of magnetic field distribution in both source and extraction regions. Thus, the external MF has the merit of gradual control of plasma parameters done precisely with keeping n_e high in the extraction region.

As is shown in Figs. 2 and 3, in hydrogen and deuterium plasmas, axial distributions of n_e and T_e are nearly equal to each other except their quantities. For reference, a typical example for axial distributions of n_e and T_e is shown in Fig. 5, where B_{MF} = 80 G. In general, both n_e and T_e in deuterium plasmas is higher than ones in hydrogen plasmas. When B_{MF} = 60 G, n_e is slightly higher than that for the case of 80 G. T_e in H_2 plasma is equal to or lower than 1 eV, but T_e in D_2 plasma is above 1eV in the extraction region. Then, plasma conditions are good for H^- production, but not good for D^- production. When B_{MF} = 80 G, values of n_e and T_e in D_2 plasmas are higher than ones in H_2 plasmas. T_e in the extraction region is decreased below 1 eV in both H_2 and D_2 plasmas. Plasma conditions are good for H^- and D^- production. The stronger MF field is required for control of T_e in D_2 plasmas. Therefore, plasma productions of H_2 and D_2 plasmas are different from each other. Thus isotope effect of plasma production is observed.

Relationship between these plasma parameter distributions and H^-/D^- production is not well clarified. The variations of H^- and D^- production due to changes in plasma parameter distributions are discussed by taking into account main collision processes for production and destruction. Dissociative attachment (DA: $H_2(v'') + e \rightarrow H^- + H$) is main process for H^- production and electron detachment (ED: $H^- + e \rightarrow H + 2e$) is main process for H^- destruction. These two processes are also applicable to the main process in D_2 plasmas for D^- production and destruction. In the following discussion, it is assumed that only $H_2(v''=8)$ or $D_2(v''=12)$ is present. $H_2(v''=8)$ and $D_2(v''=12)$ have almost the same internal energy [12]. The values of rate coefficient, $<\sigma v>_{DA}$ for DA and $<\sigma v>_{ED}$ for ED, and collision frequency, $n_e<\sigma v>_{DA}$ and $n_e<\sigma v>_{ED}$ are estimated by using measured values of T_e and n_e shown in Figs. 2 and 3.

Figure 6 and 7 show axial distributions of rate coefficients and collision frequencies of DA and ED processes, in H_2 plasmas and in D_2 plasmas, respectively [9, 10]. With changing T_e distributions, as shown in Figs. 6(a) and 7(a), distributions of ED processes are changed strongly while DA processes keep nearly the same value. It is found that T_e control by varying the intensity of the MF reduces the ED process remarkably. As shown in Figs. 6(b) and 7(b), by taking into account both T_e and n_e changes, the difference between DA with 150 G and one with 80 G is caused by n_e in this region (n_e with 80 G is higher than one with 150 G).

3.2 Production and extraction of negative ions

As shown in Figs. 2 and 3, plasma parameters in the extraction region depend strongly on the MF intensity. Figure 8 shows pressure dependence of extracted negative ion currents from (a) H_2 and (b) D_2 plasmas [8]. The negative ion currents are also strongly dependent on the MF intensity. In both cases, there are some optimum pressures. With increasing gas pressure, negative ion currents (i.e. the H^- current, I_{H^-} and the D^- current, I_{D^-}) increase in their magnitude, reach the maximum value, and then, decrease. Decreasing MF intensity, the optimum pressure p_{opt} shifts to higher pressure. For D^- production, p_{opt} is from 2 to 3.5 mTorr. On the other hand, for H^- production, p_{opt} is from 1.5 to 2 mTorr. Optimum pressure in D_2 plasmas is slightly higher than one in H_2 plasmas.

H^- density distributions across the MF are measured and its dependence on plasma parameters are studied. Figure 9 shows axial distributions of H^- ion densities, where B_{MF} = 150 G and 80 G, respectively [9, 10]. Plasma parameters corresponding to these H^- ion densities are shown in Fig. 2. Spatial distributions of H^- densities are varied by changing plasma parameters. When B_{MF} = 150 G, H^- density distribution decreases toward the extraction hole (i.e. z = -2.5 cm). On the other hand, when B_{MF} = 80 G, H^- density distribution remains nearly constant value although n_e decreases toward to the extraction hole. In front of the extraction hole (i.e. plots at z = -1.5 cm), H^- density with 80 G is higher than that with 150 G by a factor about 2. As is shown in Fig. 8, extracted H^- currents from the source are also the same ratio. Extracted H^- currents depend on H^- densities in front of the extraction hole.

D^- density distributions are compared to H^- density distributions in the same discharge condition. Figure 10 shows axial distributions of negative ion densities, where B_{MF} = 80 G, $p(H_2) = p(D_2)$ = 1.5 mTorr, respectively [9, 10]. Axial distribution of D^- density is lower than that of H^- density. According to the plasma conditions shown in Figs. 2 and 3, T_e in D_2 plasma is higher than that in H_2 plasma. With discussion described above, influence of D^- destruction by ED process on D^- density is higher although n_e in D_2 plasma is also higher. As shown in Fig. 8, extracted D^- current is also lower than H^- current, and the ratio of H^- to D^- current is almost the same as the ratio of H^- to D^- density in front of the extraction hole. Therefore, extracted D^- current is mainly determined by D^- density in front of the extraction hole. Detailed discussions in relation to negative ions in the source and extracted negative ion currents will be done below.

The relationship between the behavior of negative ions (corresponding to negative ion densities) in the source and the extracted negative ion currents are not well studied. Figure 11 shows axial distributions of negative ion densities in the source, where the field intensity of the MF is 80 G, $p(H_2)$ = 1.5 mTorr and $p(D_2)$ = 3 mTorr, respectively [8]. These two different pressure conditions correspond to the results in Fig. 8. As shown in Fig. 11, the negative ion densities in front of the extraction hole in D_2 plasmas nearly equal to that in H_2 plasmas. On the other hand, according to the results in Fig. 8, I_{D^-} at 3 mTorr with 80G is lower than I_{H^-} at 1.5 mTorr, where the same extraction voltage V_{ex} is applied for H^- extraction and D^- extraction, respectively. Considering the factor of $\sqrt{2}$ due to mass difference, $\sqrt{2}$ times I_{D^-} is nearly equal to I_{H^-}. Then D^- ion density in the source are expected to be the same as H^- ion density. Results in Fig. 11 support this.

Figure 12 shows pressure dependence of (a) D^- ion densities in the source and (b) extracted D^- currents, where the intensity of the MF is a parameter. As a whole, the patterns of pressure dependence in D^- ion densities are nearly the same as those in extracted D^- currents. Namely, the extracted D^- currents are proportional to the D^- densities in the source. According to the results shown in Figs. 9-12, the values of extracted negative ion currents are mainly determined by the negative ion densities in front of the plasma grid.

3.3 VUV emission measurement

As discussed above, plasma parameters, H^- densities and extracted H^- currents are sensitively changed by varying the magnetic field intensity of the MF. Here, we discuss the relationship between H^- production and H_2 (v”) production with measurement of VUV emission.

Figure 13 show the typical VUV spectra from both (a) H_2 and (b) D_2 plasmas. Intensity with 121.6 nm in H_2 plasmas is the spectrum of Lyman α. Because H and D are isotope, we believe that the spectrum of Lyman α from D_2 plasmas is nearly equal to that from H_2 plasmas as shown in Fig. 2(b). According to the numerical results [2], H_2 (v” ≥ 5) are more effective for H^- production. In Fig.2 (a), spectra leading to production of H_2 (v” ≥ 5) are ranged from 117.5 to 165 nm [4]. Internal energy of deuterium molecules D_2 (v” ≥ 8) are the same as that of H_2 (v” ≥ 5). Therefore, discussion on VUV spectra in H_2 plasmas should be also applicable for discussion on VUV spectra in D_2 plasmas. Namely, production of highly vibrationally excited deuterium molecules D_2 (v”) is related to the emission with the same wavelength range, i.e. 117.5 ~ 165 nm. We obtain the total intensity of the VUV spectra by integrating from 110 to 170 nm in both H_2 and D_2 plasmas. In integration of VUV spectra, Lyman α is excluded because it is not concerned with production of negative ions. In the following paragraphs, these integrated intensities are presented for discussing production of H_2 (v”) and D_2 (v”).

Figure 14 shows pressure dependence of integrated intensities of VUV spectra from H_2 plasmas, where the intensity of the MF is a parameter. Plasma parameters, H^- densities and extracted H^- currents corresponding to those VUV emissions are shown in Figs. 2, 8(a) and 9, respectively. VUV emissions are gradually increased with gas pressure. The values of integrated intensities with 150 G are highest in entire gas pressure, and intensities are decreased with the magnetic field intensity of the MF. On the other hand, as shown in Fig. 8(a), extracted H^- currents, in relation to plasma parameter control with the use of the MF, has a certain optimum pressure (i.e. 1.5 - 2 mTorr) and the values of ones are increased with a decrease in the MF intensity. Therefore, by varying the magnetic field intensity of the MF, the relation between characteristic features of VUV emissions and that of extracted H^- currents is opposite. From the behaviors of primary fast electrons in Fig. 4, the trajectories of these electrons with the case of 150 G are limited around the filaments due to stronger magnetic field. It is expected, according to the numerical results [13], that VUV emissions associated with the process (1b) occurs more frequently than that of 80 G. We have also confirmed that there are same tendencies on the discharge power dependences between VUV emissions and H^- currents among above-mentioned MF intensities.

VUV emissions from D_2 plasmas are measured to discuss the production of D_2 (v”). Figure 15 shows pressure dependence of integrated intensities of VUV spectra from H_2 and D_2 plasmas, where B_{MF} = 80 G. While difference of integrated intensities between H_2 and D_2 plasmas have little bit increase with gas pressure, ratio of the VUV emission from D_2 to H_2 plasmas are about 0.9 ~ 0.95. VUV emissions from D_2 plasmas are almost the same value or slightly lower than ones from H_2 plasmas. On the other hand, the ratio of reported cross section of D_2(v”) to H_2(v”) production [14] are about 0.7. The ratio of measured values of VUV emissions and ratio of cross sections are different from each other.

According to the results of the H^- and D^- ions extraction shown in Fig. 8, characteristics of extracted H^- and D^- currents are quite different from each other. The values of extracted H^- currents are sensitively increased with decreasing the magnetic field intensity of the MF. On the other hand, the extracted D^- currents are not so increased under the same discharge conditions with H_2 plasmas. In the future, VUV emissions from H_2 and D_2 plasmas will be compared to discuss the difference of characteristic features of extracted H^- and D^- currents. We have confirmed numerically that extraction probability of negative ions depends strongly on upstream distance from the extraction grid [15]. At any rate, to increase the extraction of negative ion currents, production of negative ions near the extraction grid should be enhanced by optimizing plasma conditions.

4. Summary

Production and control of plasma parameters in H_2 and D_2 plasmas are performed by varying the intensity of the MF. The values of T_e and n_e in D_2 plasmas are slightly higher than ones in H_2 plasmas. T_e in D_2 plasmas cannot be decreased and is kept above 1 eV in the extraction region with the same MF intensity for optimizing H_2 plasmas. The stronger MF field is required for control of T_e in D_2 plasmas. Therefore, plasma production between H_2 and D_2 plasmas is different from each other. Namely isotope effect of plasma production is observed. H^- and D^- densities have different spatial distributions corresponding to those different plasma parameters. Extracted H^- and D^- currents are mainly determined by H^- and D^- densities in front of the extraction hole, respectively. According to the discussions based on estimated rate coefficient and collision frequency of main collision processes, it is reconfirmed that T_e in the extraction region should be reduced below 1 eV with n_e keeping higher for enhancement of H^- and D^- production. For further studying enhancement of D^- production, preliminary results of simultaneous measurements of VUV emission and negative ion density in the source is presented and isotope effect of H^-/D^- volume production is briefly discussed.

Acknowledgements

The authors would like to thank Prof. Y. Takeiri and Dr. K. Tsumori (National Institute for Fusion Science) for their valuable discussions. The authors also thank Prof. H. Naitou and Y. Tauchi (Yamaguchi University) for their discussion and support in the experiments. A part of this work was supported by the Grant-in-Aid for Scientific Research from Ministry of Education, Culture, Sports, Science and Technology, Japan. This work was also performed with the support of the NIFS LHD Project Research Collaboration.

References

[1] Hiskes, J. R., and Karo, A. M., J. Appl. Phys. **56** (1984) 1927.

[2] Fukumasa, O., J. Phys. **D22** (1989)1668.

[3] Fukumasa, O., Tauchi, Y., Yabuki, Y., Mori, S., and Takeiri, Y., *Proceedings of the 9th International Symposium on the Production and Neutralization of Negative Ions and Beams* (2002) 28.

[4] Graham, W. G., J. Phys. **D17** (1984) 2225.

[5] Fukumasa, O., Mizuki, N., and Niitani, E., Rev. Sci. Instrum. **69** (1998) 995.

[6] Mori, S., Tauchi, Y., Fukumasa, O., Hamabe, M. and Takeiri, Y., *Abstracts of the 30th IEEE International Conference on Plasma Science* (2003) 209.

[7] Fukumasa, O., *Proceedings of the 26th International Conference on Phenomena in Ionized Gases* **1** (2003) 13.

[8] Fukumasa, O., Mori, S., Nakada, N., Tauchi, Y., Hamabe, M., Tsumori, K. and Takeiri, Y., Contrib. Plasma Phys. **44** (2004) 516.

[9] Mori, S., Tauchi, Y., Fukumasa, O., Hamabe, M., Tsumori, K. and Takeiri, Y., *Proceedings of the Novel Materials Processing by Advanced Electromagnetic Energy Sources 2004* (2004) (to be published).

[10] Mori, S. and Fukumasa, O., *Abstracts of 7th Asia Pacific Conference on Plasma Science and Technology and 17th Symposium on Plasma Science for Materials* (2004) 451, Thin Solid Films (2005, in press).

[11] Bacal, M. and Hamilton, G. W., Phys. Rev. Lett. **42** (1979) 1538.

[12] Wadehra, J. M., Appl. Phys. Lett. **35** (1979) 917.

[13] Mori, S. and Fukumasa, O., in preparation.

[14] Celiberto, R., Capitelli, M. and Lamanna, U. T., Chem. Phys. **183** (1994) 101.

[15] Fukumasa, O. and Nishida, R., *Proceedings of the 10th International Symposium on the Production and Neutralization of Negative Ions and Beams* (2004) 159.

Figure captions

Figure 1. Schematic diagram of the ion source. The probe, the laser path, and power meter used in photo- detachment experiments are also shown.

Figure 2. Axial distributions of plasma parameters (a) n_e and (b) T_e in H_2 plasmas. Experimental conditions are as follows: discharge voltage $V_d = 70$ V, discharge current $I_d = 5$ A, gas pressure $p(H_2) = 1.5$ mTorr. Parameter is the magnetic field intensity of the magnetic filter (MF).

Figure 3. Axial distributions of plasma parameters (a) n_e and (b) T_e in D_2 plasmas. Experimental conditions are as follows: $V_d = 70$ V, $I_d = 5$ A, $p(D_2) = 1.5$ mTorr. Parameter is the magnetic field intensity of the MF.

Figure 4. Behaviors of fast primary electrons for two different intensities of the MF: (a) 150 G and (b) 80 G.. Trajectories of 20 test particles are plotted.

Figure 5. Axial distributions of plasma parameters (a) n_e and (b) T_e in H_2 and D_2 plasmas. Experimental conditions are as follows: $V_d = 70$ V, $I_d = 5$ A, $p(H_2) = p(D_2) = 1.5$ mTorr.

Figure 6. Axial distributions of (a) rate coefficient and (b) collision frequency estimated by measured T_e and n_e in H_2 plasmas (closed circle; H^- production with 150 G, closed triangle; H^- production with 80 G, open circle; H^- destruction with 150 G, open triangle; H^- destruction with 80 G). Corresponding plasma parameters are shown in Fig. 2.

Figure 7. Axial distributions of (a) rate coefficient and (b) collision frequency estimated by measured T_e and n_e in D_2 plasmas (closed circle; D^- production with 150 G, closed triangle; D^- production with 80 G, open circle; D^- destruction with 150 G, open triangle; D^- destruction with 80 G). Corresponding plasma parameters are shown in Fig. 3.

Figure 8. Pressure dependences of extracted (a) H^- and (b) D^- currents. Experimental conditions are as follows: $V_d = 70$ V, $I_d = 5$ A, and extraction voltage $V_{ex} = 1.5$

kV. Parameter is the magnetic field intensity of the MF.

Figure 9. Axial distributions of H^- ion densities. Experimental conditions are as follows: V_d = 70 V, I_d = 5 A and $p(H_2)$ = 1.5 mTorr. Parameter is the magnetic field intensity of the MF. Corresponding plasma parameters are shown in Fig. 2 (with B_{MF} = 150 G and 80 G).

Figure 10. Axial distributions of H^- and D^- ion densities. Experimental conditions are as follows: V_d = 70 V, I_d = 5 A, $p(H_2$ or $D_2)$ = 1.5 mTorr and B_{MF} = 80 G. Corresponding plasma parameters are shown in Fig. 2 (for H_2 plasma) and Fig. 3 (for D_2 plasma).

Figure 11. Axial distributions of H^- and D^- ion densities. Experimental conditions are as follows: V_d = 70 V, I_d = 5 A, $p(H_2)$ = 1.5 mTorr, $p(D_2)$ = 3 mTorr and B_{MF} = 80 G.

Figure 12. Pressure dependences of (a) D^- ion densities in the source and (b) extracted D^- currents. Experimental conditions are as follows: V_d = 70 V, I_d = 5 A and V_{ex} = 1.5 kV. D^- ion densities are measured at z = -0.5 cm. Extraction hole is set at z = -1.5 cm. Parameter is the magnetic field intensity of the MF.

Figure 13. Typical VUV spectra from (a) H_2 and (b) D_2 plasmas. Experimental conditions are as follows: V_d = 70 V, I_d = 5 A, $p(H_2) = p(D_2)$ = 3 mTorr and B_{MF} = 80 G.

Figure 14. Pressure dependence of integrated intensities of VUV spectra from H_2 plasmas. Experimental conditions are as follows: V_d = 70 V, I_d = 5 A. Parameter is the magnetic field intensity of the MF.

Figure 15. Pressure dependence of integrated intensities of VUV spectra from H_2 and D_2 plasmas. Experimental conditions are as follows: V_d = 70 V, I_d = 5 A and B_{MF} = 80 G.

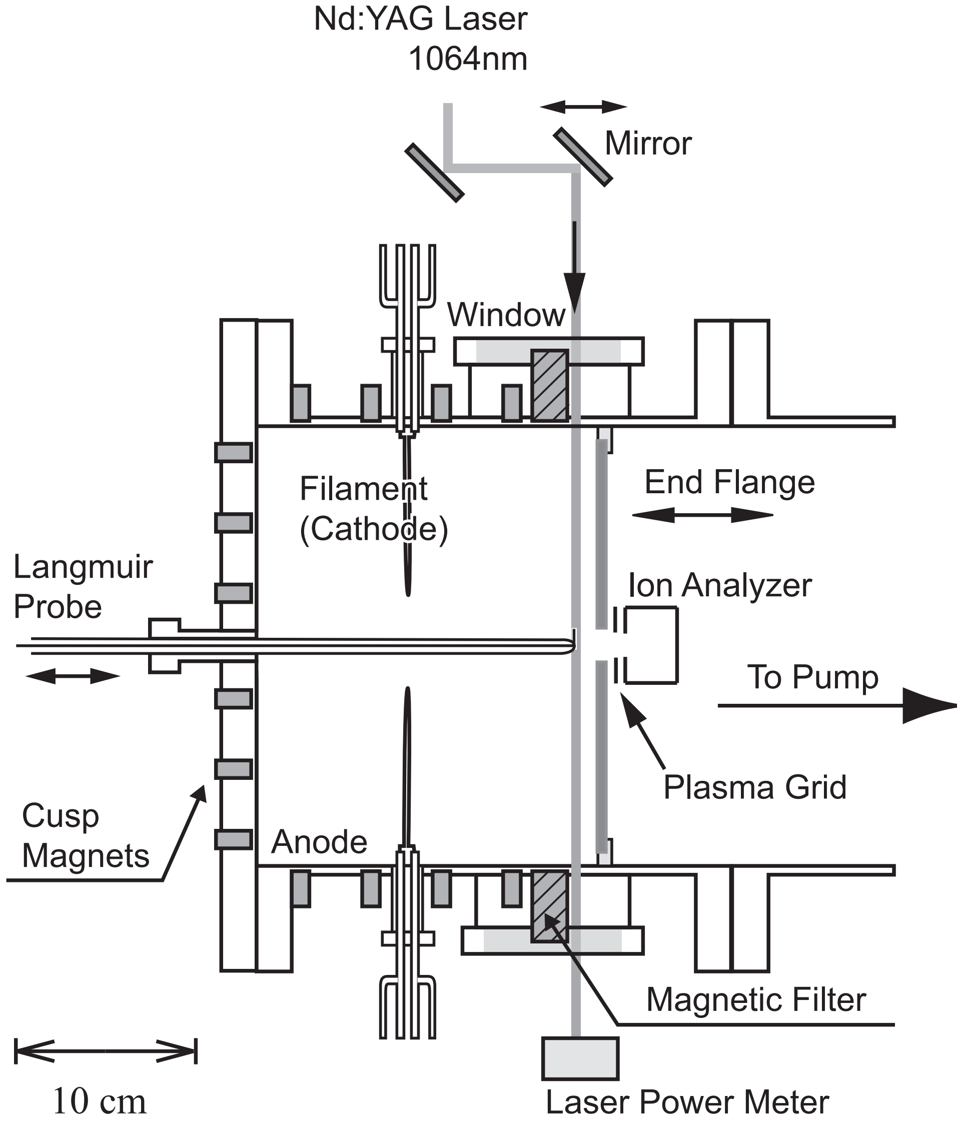

Fig. 1 O. Fukumasa

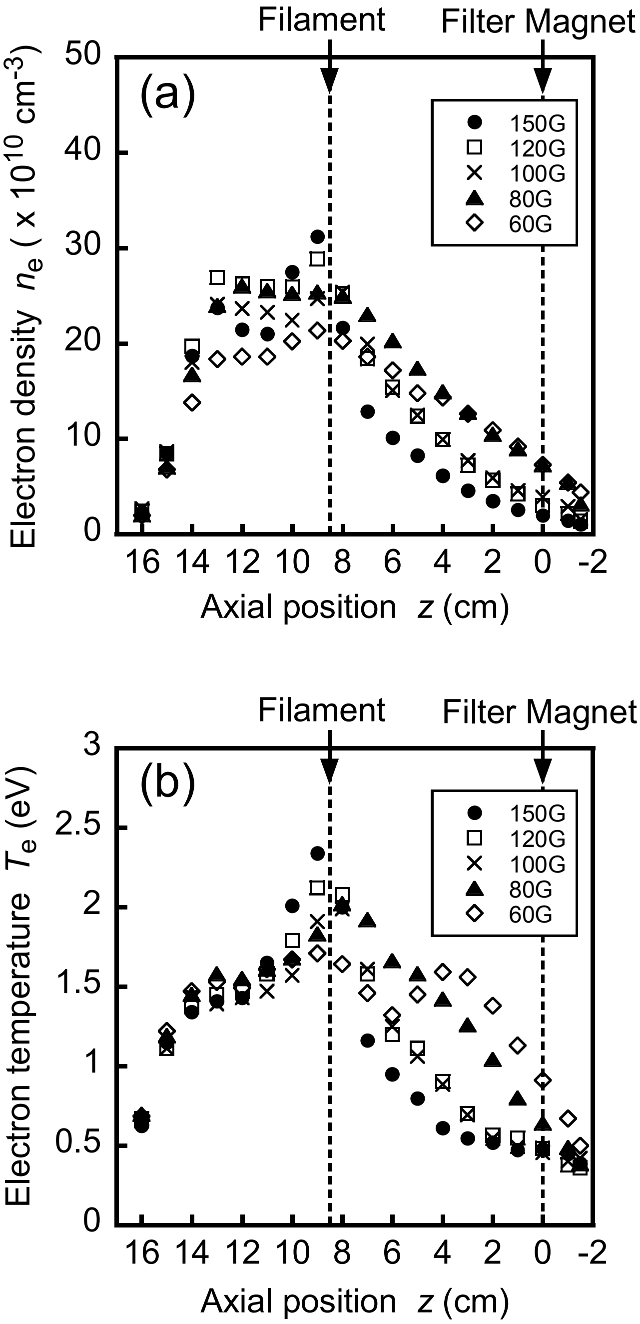

Fig. 2 O. Fukumasa

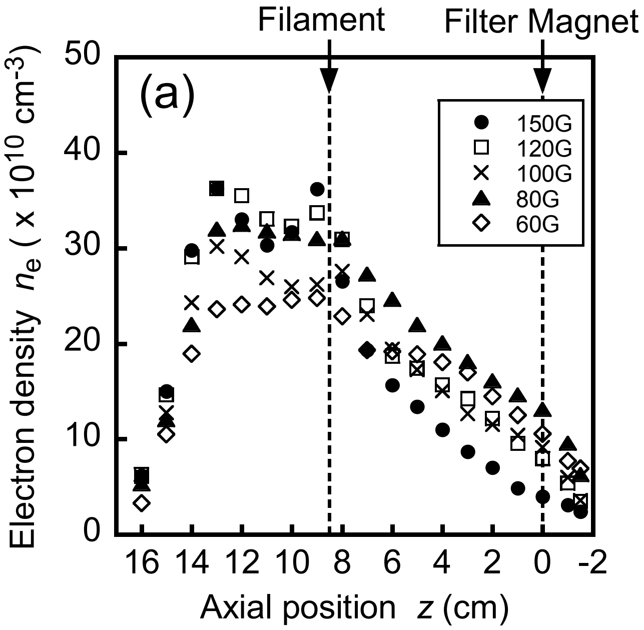

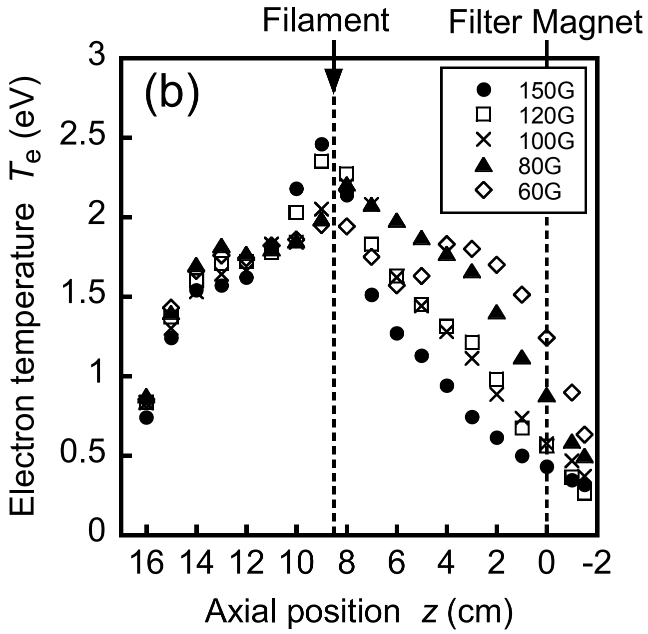

Fig. 3 O. Fukumasa

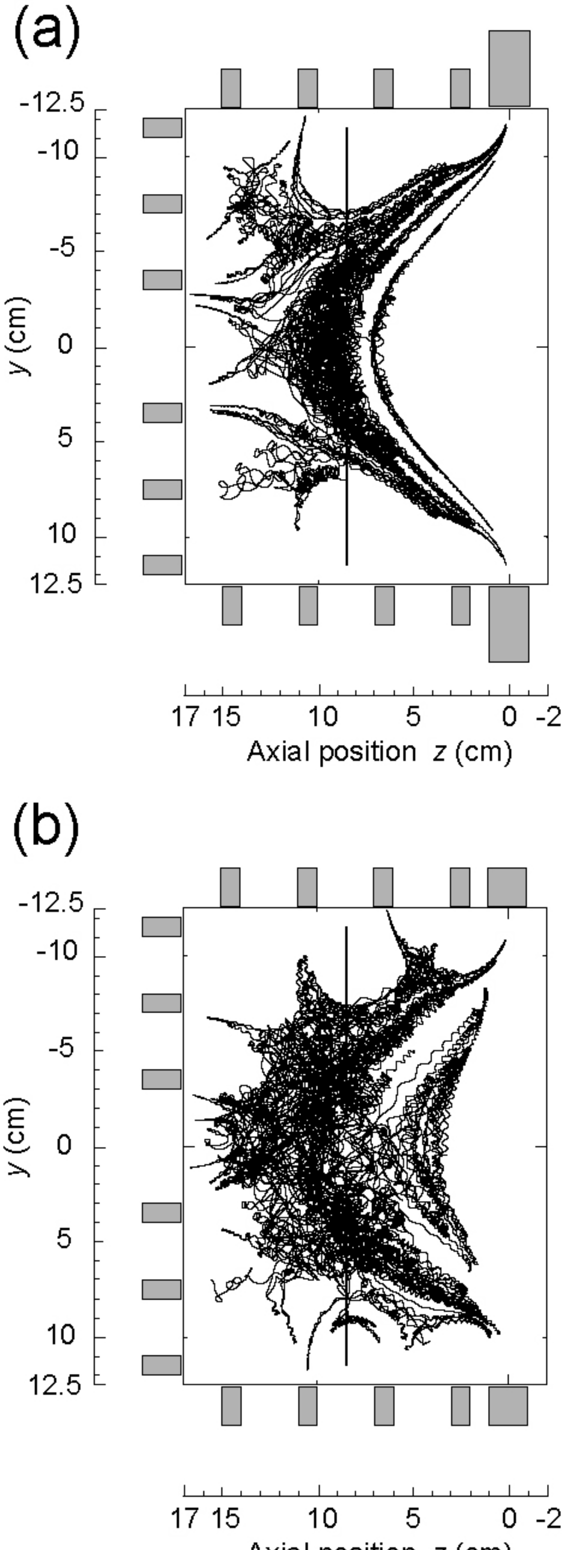

Fig. 4 O. Fukumasa

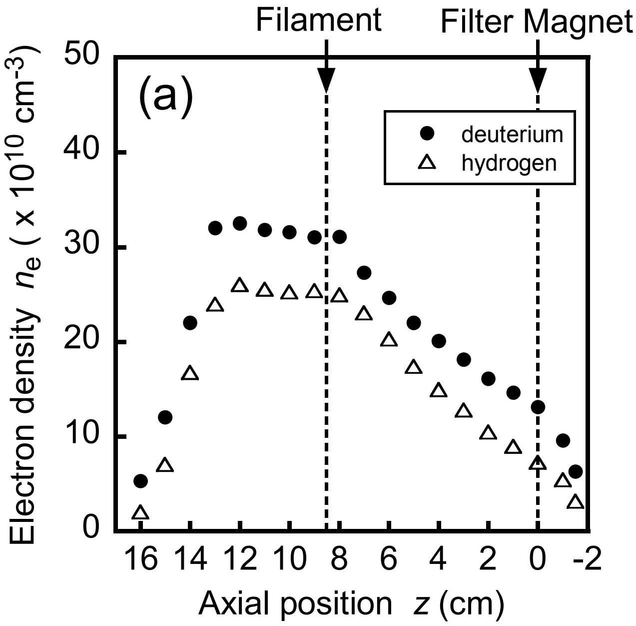

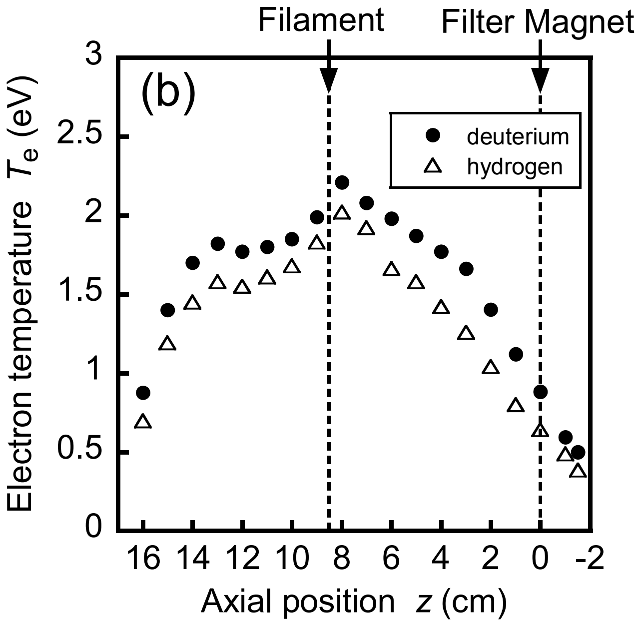

Fig. 5 O. Fukumasa

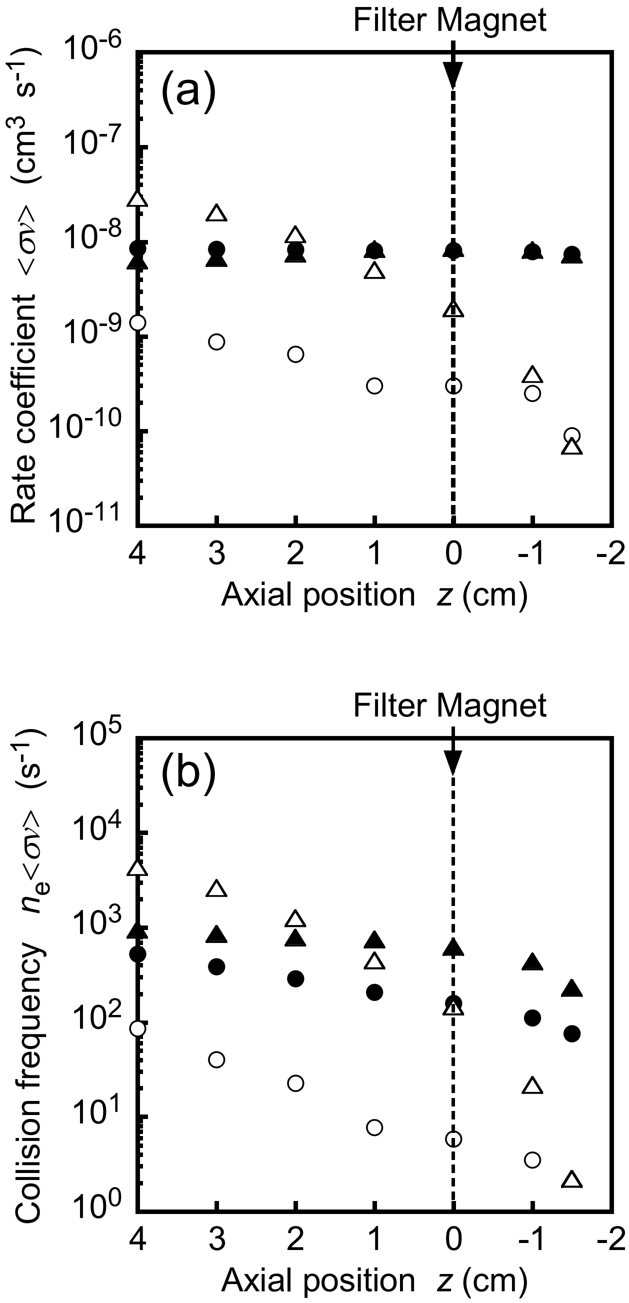

Fig. 6 O. Fukumasa

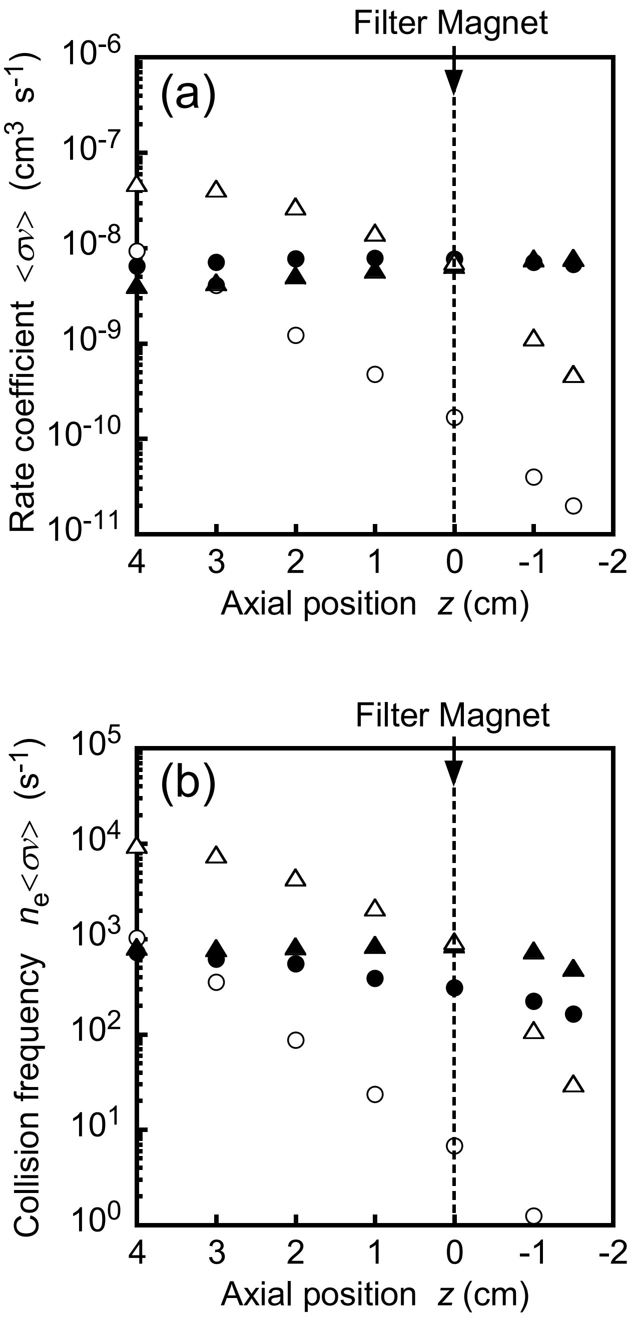

Fig. 7 O. Fukumasa

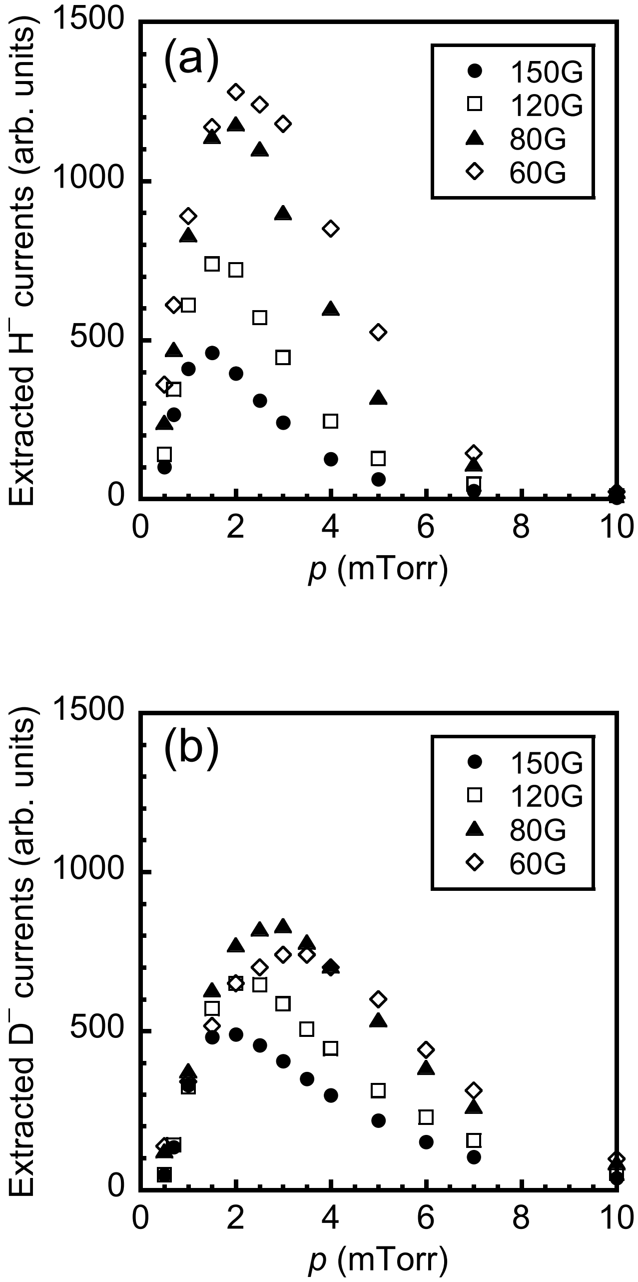

Fig. 8 O. Fukumasa

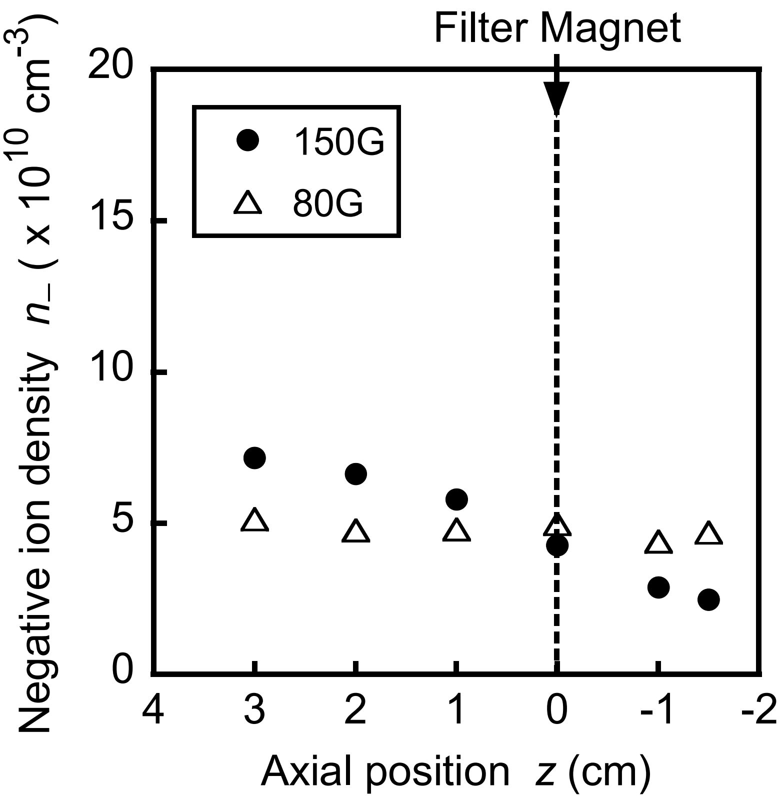

Fig. 9 O. Fukumasa

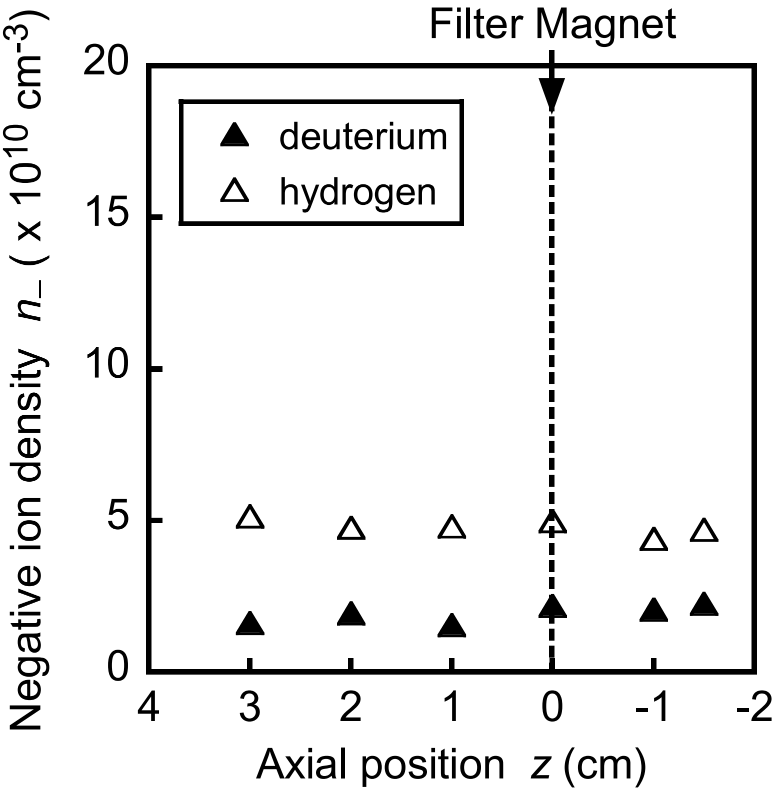

Fig. 10 O. Fukumasa

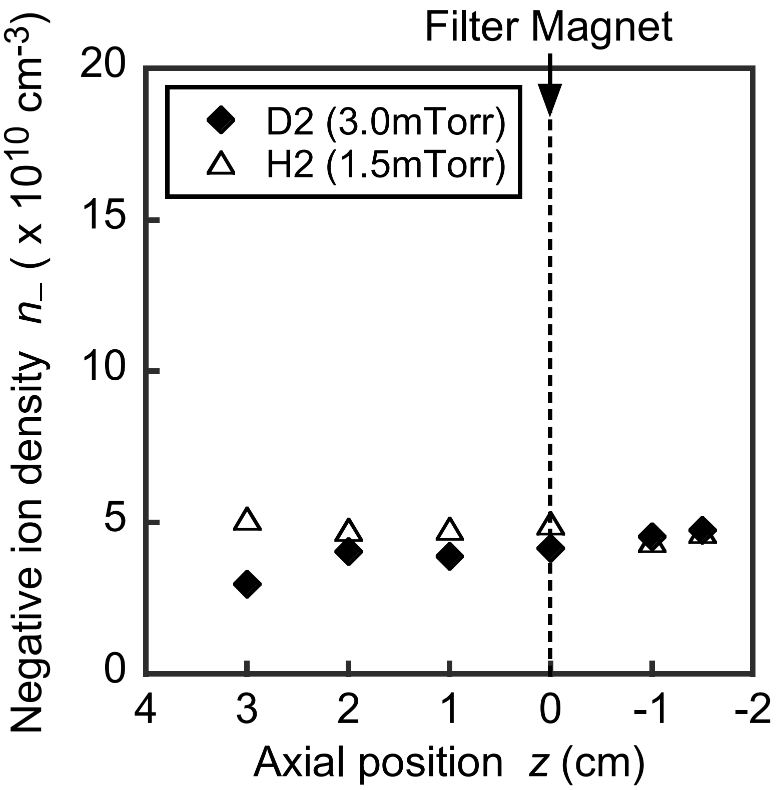

Fig. 11 O. Fukumasa

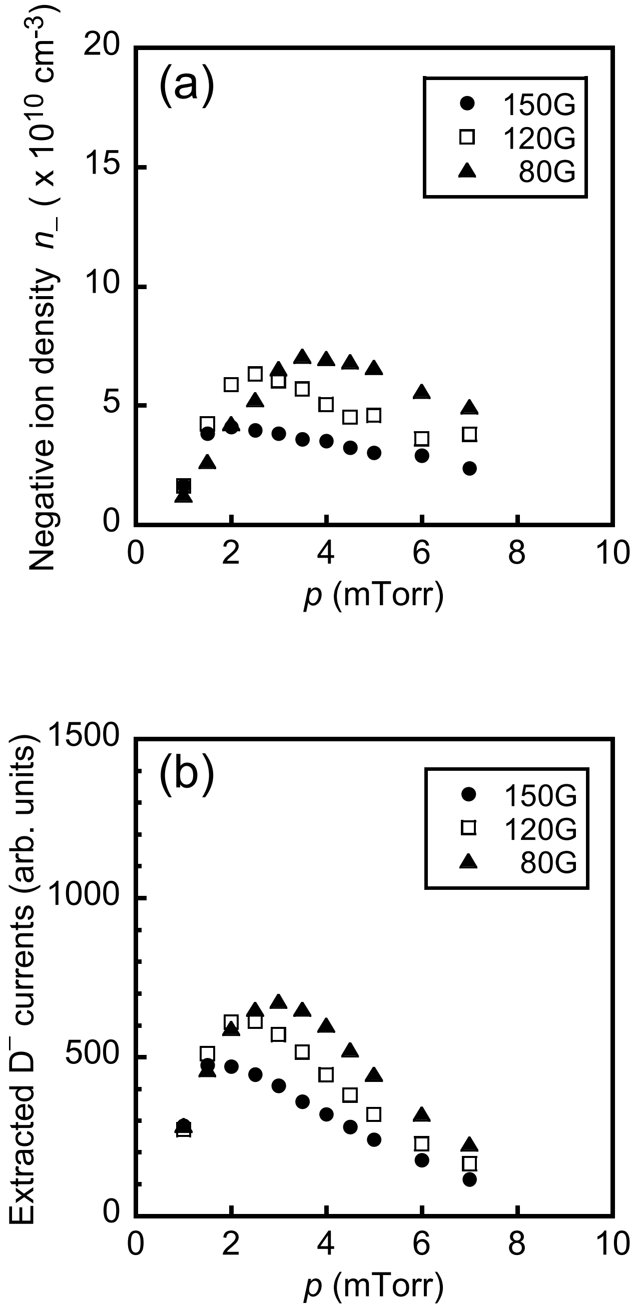

Fig. 12 O. Fukumasa

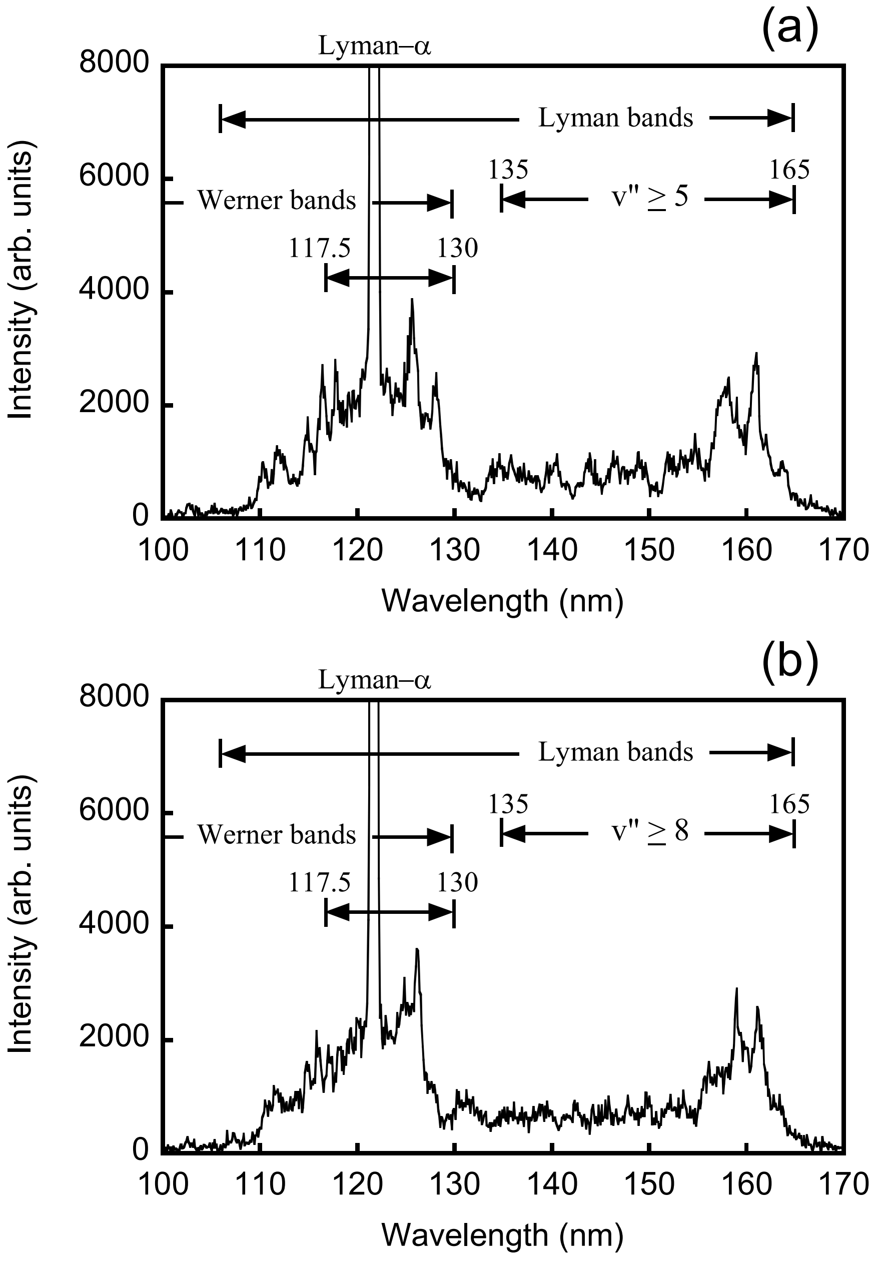

Fig. 13 O. Fukumasa

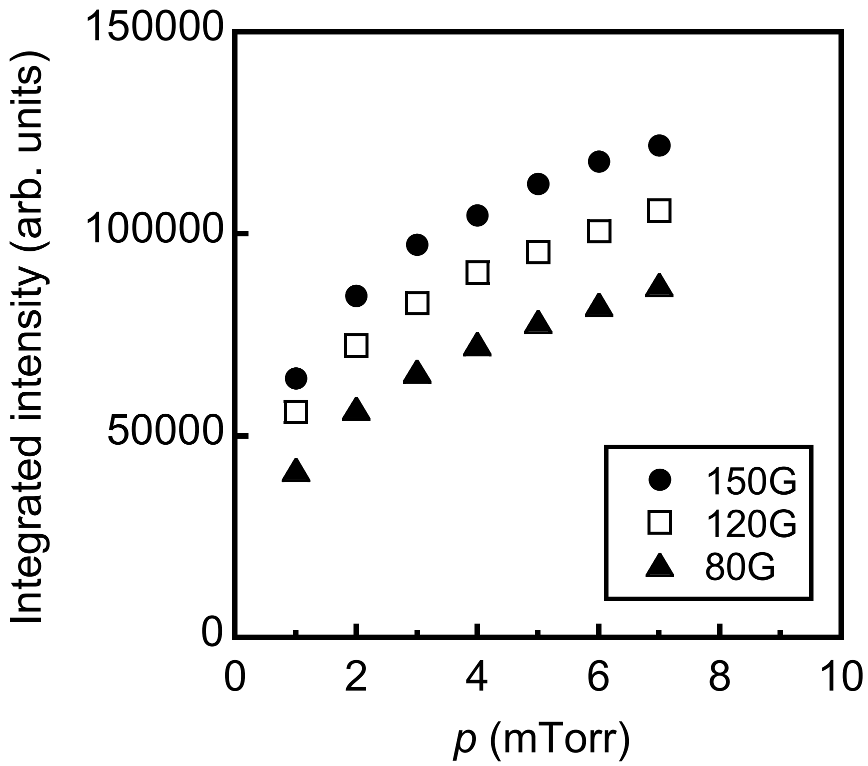

Fig. 14　O. Fukumasa

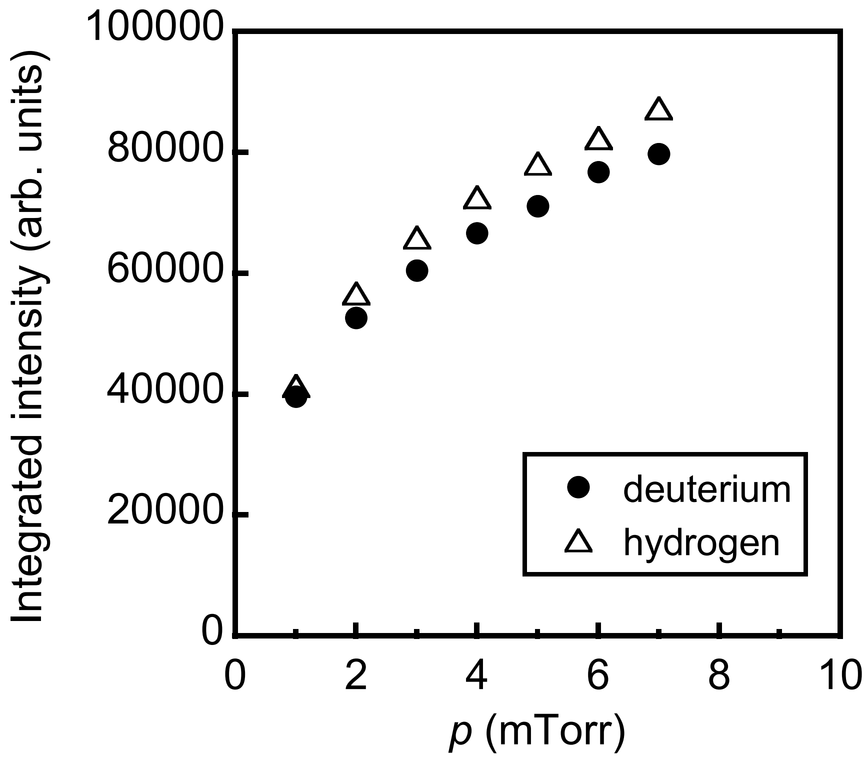

Fig. 15 O. Fukumasa